

Sol–gel derived LaFeO₃/SiO₂ nanocomposite: synthesis, characterization and its application as a new, green and recoverable heterogeneous catalyst for the efficient acetylation of amines, alcohols and phenols

Saeed Farhadi · Kosar Jahanara · Asma Sepahdar

Received: 14 August 2013 / Accepted: 1 November 2013
© Iranian Chemical Society 2013

Abstract LaFeO₃/SiO₂ nanocomposite was synthesized by the sol–gel process from metal nitrates and tetraethyl orthosilicate (TEOS) as the SiO₂ source. The nanocomposite product was characterized by XRD, FT-IR, SEM, and surface area measurements and was used as a heterogeneous catalyst for the efficient acetylation of amines, alcohols and phenols to the corresponding acetates using acetic anhydride under solvent-free conditions. Among the various substrates, acetylation of amines was preceded rapidly, so that an amine group could be selectively acetylated in the presence of alcoholic or phenolic hydroxyl groups by the appropriate choice of reaction time. The catalyst can also be reused several times without the loss of activity. In addition, the catalytic activity of the LaFeO₃/SiO₂ nanocomposite was higher than that of the pure LaFeO₃ nanoparticles. The method is high yielding, clean, cost effective, compatible with the substrates having other functional groups and very suitable for the practical organic synthesis.

Keywords Lanthanum orthoferrite · Silica matrix · Sol–gel process · Nanocomposite · Heterogeneous catalyst · Acetylation · Solvent-free conditions

Introduction

Acetylation is an efficient route for protecting the functional groups of alcohols, phenols and amines during oxidation, peptide coupling and glycosidation reactions [1, 2]. Numerous catalytic systems are available for this important

organic transformation [3–13], but most of them are homogeneous and non-recoverable. In addition, many of these methods have certain drawbacks, such as long reaction time, involvement of toxic and expensive reagents, use of additional reagents, requirement of special effort for catalyst preparation, need to use special apparatus, moderate yields, and side reactions. With growing environmental concerns, much attention has been directed towards this transformation using heterogeneous catalysts [14, 15]. Heterogeneous catalysts can be easily recovered from reaction mixture by simple filtration and can be reused several times, making the process more economically and environmentally viable. In this context, heterogeneous catalysts such as HClO₄–SiO₂ [16], montmorillonites [17–19], metal oxides [20–22], H₂SO₄–SiO₂ [23], zeolites [24, 25], HBF₄–SiO₂ [26], MoO₃–Al₂O₃ [27], NaHSO₄–SiO₂ [28], sulphated zirconia [29], (NH₄)_{2.5}H_{0.5}PW₁₂O₄₀ [30], silica-bonded cobalt(II) salen [31], silica-bonded *N*- and *S*-propyl sulfamic acids [32, 33], poly(4-vinylpyridinium) perchlorate [34], polystyrene-supported GaCl₃ [35], borated zirconia modified with ammonium metatungstate [36] and rice husk [37] have been applied for the acetylation of alcohols and phenols. However, each of these catalysts has advantages and limitations.

In recent years, transition metal mixed oxides with perovskite-type structure (ABO₃) have attracted considerable attention as promising catalytic materials for organic transformations due to their high thermal and hydrothermal stability and relatively low cost compared with their conventional noble metal counterparts [38–43]. However, the potential catalytic applications of them are greatly limited by their low surface areas. One possible way of circumventing this problem is to disperse these oxides in a medium that possesses a high-specific surface area. The sol–gel technique has been widely used as an appropriate method for preparing various nanostructured materials and nanocomposites [44, 45]. In

S. Farhadi (✉) · K. Jahanara · A. Sepahdar
Department of Chemistry, Lorestan University,
68135-465 Khorramabad, Iran
e-mail: sfarhadi48@yahoo.com

comparison with traditional method, the sol–gel method offers the advantage of good chemical homogeneity and high purity. In addition, sol–gel derived nanocomposite can be obtained at a temperature much lower than that necessary for the melting of an oxide mixture. Silica-based nanomaterials have been reported to be promising supports for a number of catalytically active species because of their high surface area and stable well-ordered pore structures [46–48].

In this paper, perovskite-type lanthanum orthoferrite (LaFeO_3) nanoparticles embedded in silica matrix (abbreviated as $\text{LaFeO}_3/\text{SiO}_2$ nanocomposite) were easily prepared via a sol–gel process and its catalytic activity was evaluated for the acetylation reaction with acetic anhydride as a protecting agent. The results indicate that the $\text{LaFeO}_3/\text{SiO}_2$ nanocomposite is a selective and highly efficient recyclable catalyst for the acetylation of alcohols, phenols and amines to the corresponding acetates under solvent-free conditions. To the best of our knowledge, this is the first report of the catalytic reaction of organic compounds over a perovskite-type mixed oxide-silica nanocomposite.

Experimental

General

The reagents used in the synthesis of LaFeO_3 embedded in silica matrix were $\text{Fe}(\text{NO}_3)_3 \cdot 9\text{H}_2\text{O}$ (98 %), $\text{La}(\text{NO}_3)_2 \cdot 6\text{H}_2\text{O}$ (99 %) and tetraethyl orthosilicate $\text{Si}(\text{OC}_2\text{H}_5)_4$ (TEOS >99.5 %), which were purchased from Merck chemical Co. All chemicals and solvents were purchased from Merck in the highest purities available (>98 %) and used as received. $^1\text{H-NMR}$ spectra were recorded on a Bruker 500 MHz instrument. GC–MS analysis was carried out on a Shimadzu QP 5050 GC–MS instrument. The $\text{LaFeO}_3/\text{SiO}_2$ nanocomposite was characterized by a Bruker D8 Advance X-ray diffractometer using $\text{CuK}\alpha$ radiation ($\lambda = 1.5406 \text{ \AA}$). Infrared spectra were recorded on a Shimadzu system FT-IR 8400 spectrophotometer using the KBr pellet method. The particle size and morphology of the $\text{LaFeO}_3/\text{SiO}_2$ nanocomposite were investigated by LEO-906E transmission electron microscope (TEM) with an accelerating voltage of 80 kV. In the process of preparation of the TEM specimen, a small amount of the powders was dispersed in ethanol in an ultrasonic bath for 30 min, and few drops the resulting suspension were placed onto a carbon coated copper grid. The specific surface area of the catalyst was calculated by the Brunauer–Emmett–Teller (BET) method using N_2 adsorption–desorption experiments carried out at $-196 \text{ }^\circ\text{C}$ on a surface area analyzer (Micromeritics ASAP 2010). Before each measurement, the sample was degassed at $200 \text{ }^\circ\text{C}$ for 1 h.

Catalyst preparation and characterization

$\text{LaFeO}_3/\text{SiO}_2$ nanocomposite containing 40 % w/w LaFeO_3 was synthesized on the basis of sol–gel method as follows. A mixture of TEOS (23.5 mL; SiO_2 content: 6.3 g), ethanol (50 mL) and water (10 mL) was prepared in a 250-ml beaker. The mixture was stirred at room temperature for 1 h. Then, a mixture of $\text{Fe}(\text{NO}_3)_3 \cdot 9\text{H}_2\text{O}$ (7 g) and $\text{La}(\text{NO}_3)_2 \cdot 6\text{H}_2\text{O}$, (7.5 g) dissolved in water (40 mL) was added. The resulting mixture was stirred for 1 h and allowed to gel at room temperature within 5 days. After gelation, it was dried and calcined at 300, 400 and $500 \text{ }^\circ\text{C}$ for 4 h and washed with hot water ($80 \text{ }^\circ\text{C}$) three times to give ca. 10 g of the $\text{LaFeO}_3/\text{SiO}_2$ nanocomposite. On the basis of the solid mass obtained at the end of the preparation at $500 \text{ }^\circ\text{C}$ and the initial amount of two metal nitrates employed, we could estimate that the prepared material, $\text{LaFeO}_3/\text{SiO}_2$, contained 40 % (w/w) of LaFeO_3 . A SiO_2 sample not including LaFeO_3 was also prepared, following the procedure described above but without adding the two metal nitrates. In addition, pure LaFeO_3 nanoparticles were prepared according to the previous method by us and its catalytic activity was compared with LaFeO_3 nanoparticles embedded in an inert matrix [49].

General procedure for the acetylation reaction on $\text{LaFeO}_3/\text{SiO}_2$ nanocomposite

To a mixture of the $\text{LaFeO}_3/\text{SiO}_2$ nanocomposite (0.25 g) and acetic anhydride (2 mmol), alcohol, phenol and/or amine (2 mmol) were added. The mixture was stirred, and the progress of the reaction was monitored by TLC. After an appropriate time when the reaction was completed, 10 mL of ethyl acetate and/or diethyl ether was added and the mixture was filtered to separate the catalyst. The catalyst was washed with ethyl acetate ($2 \times 7.5 \text{ mL}$) for recycling. The combined organic phases were washed with 10 % solution of sodium hydrogen carbonate and dried over MgSO_4 . The solvent was removed to afford the product. If further purification was needed it was passed through a short column of silica gel. All products were characterized on the basis of GC–MS, FT-IR and $^1\text{H-NMR}$ spectral data and comparison with those of authentic samples or reported data. The results are summarized in Tables 1–5.

Results and discussion

Characterization of $\text{LaFeO}_3/\text{SiO}_2$ nanocomposite

Figure 1 shows the XRD patterns of the $\text{LaFeO}_3/\text{SiO}_2$ gels heat-treated at $300\text{--}500 \text{ }^\circ\text{C}$ temperature range for 4 h.

Table 1 The effect of LaFeO₃/SiO₂ nanocomposite amount on the reaction of benzyl alcohol with acetic anhydride

Entry	Catalyst (g)	Solvent	Time (min)	Yield ^a (%)
1	0.05	–	25	14
2	0.10	–	25	18.5
3	0.15	–	25	42
4	0.20	–	25	76
5	0.25	–	18	90
6	0.30	–	18	88
7	0.25	Acetonitrile	30	35
8	0.25	Toluene	30	15
9	0.25	Dichloromethane	30	26
10	0.25	Acetone	30	40
11 ^b	0.10	–	30	15
12 ^c	0.15	–	30	Trace
13	–	–	30	Trace

Reaction conditions: benzyl alcohol (2 mmol); acetic anhydride (2 mmol) without solvent at r.t. or with solvent (10 mL) under refluxing conditions

^a Isolated yield

^b Unsupported LaFeO₃ (0.10 g) used as the catalyst, without solvent at r.t.

^c SiO₂ used as the catalyst, without solvent at r.t.

From the Fig. 1a, it is clear that the gel sample calcined at 300 °C is amorphous, with one broad reflection centered at approximately $2\theta = 22.5^\circ$, which is characteristic of diffraction of the amorphous SiO₂ matrix. As can be seen in Fig. 1b and c, heating beyond 300 °C resulted in a gradual crystallization of the samples. Increase of heat-treated temperature to 400 and then 500 °C was resulted in an increase in crystallinity. All peaks indexed as (2 2 0), (3 1 1), (4 0 0), (4 2 2), (5 1 1) and (4 4 0) in XRD patterns were assigned to the LaFeO₃ phase (ICCD Card File No. 5-0669), no other crystalline phases were detected in the calcined samples. In the XRD patterns, broad humps are present at approximately $2\theta = 22.5^\circ$, which can be attributed to the amorphous phase of SiO₂ matrix. This means that the materials consist of the LaFeO₃ nanoparticles and an amorphous phase of SiO₂. Further, the diffraction peaks of the LaFeO₃ phase are markedly broadened due to the small size effect of the particles. The average particle size can be calculated by X-ray diffraction line broadening using the Debye–Scherrer equation [50]: $d = (0.9\lambda)/(h_{1/2}\cos\theta)$, where d represents the grain size; λ is the wavelength of the X-ray (CuK_α, 1.5406 Å); θ is the diffraction angle of the peak; and $h_{1/2}$ stands for the full width at half height of the peaks. The average particle size calculated using the most intense peak (3 1 1) at $2\theta = 36.90^\circ$ is approximately 15 nm. This value is consistent with the TEM observations (discussed below).

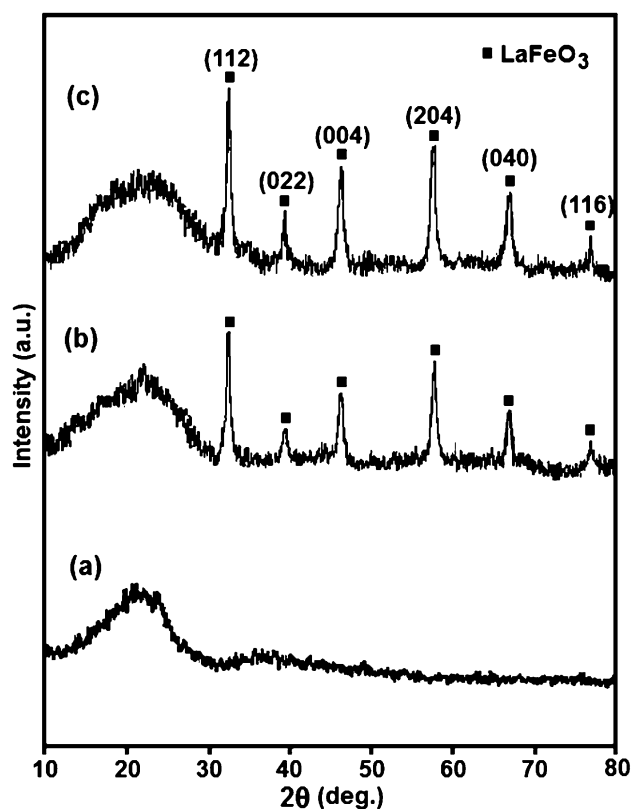


Fig. 1 XRD patterns of LaFeO₃/SiO₂ samples calcined at different temperatures for 4 h: **a** 300 °C, **b** 400 °C, and **c** 500 °C

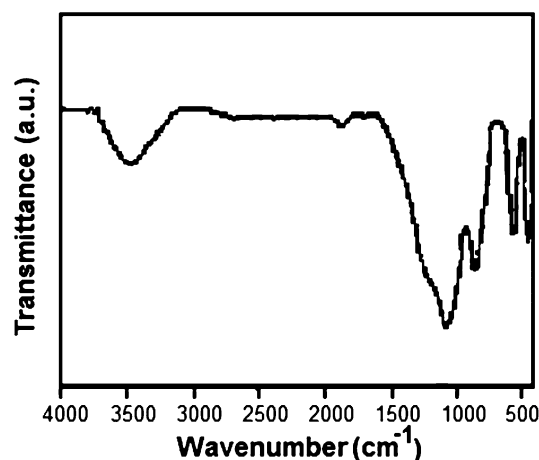


Fig. 2 FT-IR spectrum of the LaFeO₃/SiO₂ nanocomposite prepared at 500 °C

The XRD analysis confirmed that high crystalline LaFeO₃/SiO₂ nanocomposite was completely formed by calcining the dried gel at 500 °C for 4 h, for further confirmation of its structure the FT-IR spectrum of this sample was recorded. As shown in Fig. 2, the bands centered at 1,078 and 800 cm⁻¹ correspond to the stretching and bending vibrations of Si–O–Si bonds of the silica network

formed via the hydrolysis and polycondensation reactions of the $\text{Si}(\text{OEt})_4$ precursor [51]. In addition, two sharp bands that appeared around 570 and 425 cm^{-1} are related to the Fe–O stretching and O–Fe–O bending vibrations of the FeO_6 octahedron group in the perovskite-type LaFeO_3 structure, respectively [52]. This finding proves the formation of the perovskite-type LaFeO_3 in the silica network in agreement with the XRD data.

In Fig. 3, the TEM image of the $\text{LaFeO}_3/\text{SiO}_2$ nanocomposite obtained by calcining the corresponding gel at $500\text{ }^\circ\text{C}$ was presented. The dark and semi-spherical particles in the TEM image are LaFeO_3 nanoparticles. From the TEM image, we observe that LaFeO_3 is present as nanoparticles homogeneously distributed in the silica matrix with the particles size up to 25 nm. As can be seen, a large amount of the LaFeO_3 nanoparticles is embedded in amorphous SiO_2 matrix. The LaFeO_3 nanoparticles possess a narrow size distribution in a range from 10 to 25 nm, and the mean particle diameter is about 17 nm. This value is consistent with the average size of the crystallites calculated from the XRD pattern using the Scherrer equation (discussed above).

The catalytic activity of a heterogeneous nanocatalyst is also dependent on its surface properties. N_2 adsorption–desorption isotherms were conducted to investigate the surface area of the $\text{LaFeO}_3/\text{SiO}_2$ nanocomposite. As shown in Fig. 4, the surface area of the $\text{LaFeO}_3/\text{SiO}_2$ nanocomposite calculated by the BET method is $166.40\text{ m}^2/\text{g}$, which is much higher than that of the pure LaFeO_3 nanoparticles ($38.5\text{ m}^2/\text{g}$) [49]. The high-specific surface area of the nanocomposite product also indicated the possibility of its application as an efficient catalytic material. The isotherm curve is close to Type IV of the IUPAC classification with an evident hysteresis loop in the 0.5–1.0 range of relative pressure, indicating that the existence of the SiO_2 network prevented the LaFeO_3 nanoparticles from

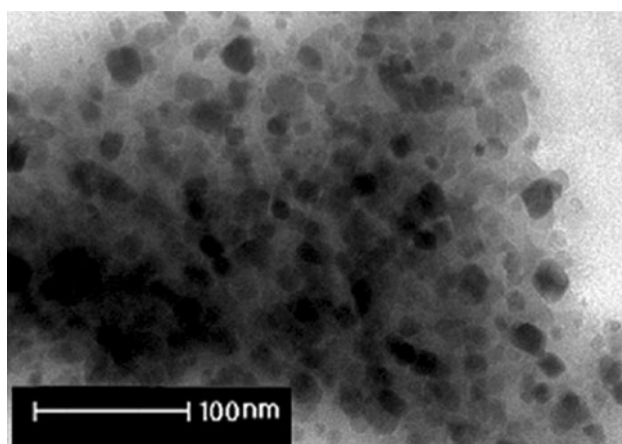


Fig. 3 TEM image of the $\text{LaFeO}_3/\text{SiO}_2$ nanocomposite prepared at $500\text{ }^\circ\text{C}$

aggregating, which was expected to improve the catalytic activity of the LaFeO_3 dispersed in the SiO_2 matrix. Meanwhile, the shape of the hysteresis loop confirms that the nanocomposite sample under study is basically mesoporous.

The acetylation reaction over the $\text{LaFeO}_3/\text{SiO}_2$ nanocomposite

The activity of the as-prepared $\text{LaFeO}_3/\text{SiO}_2$ nanocomposite as a novel heterogeneous catalyst in the acetylation of alcohols, phenols and amines was investigated. At the outset, we carried out the optimization reactions to find out the best conditions using benzyl alcohol as a model substrate. A mixture of benzyl alcohol (2 mmol) and acetic anhydride (2 mmol) in the presence of various amounts of the catalyst was stirred at room temperature under solvent-free conditions. The progress of the reaction was monitored by TLC. The isolated yield of benzyl acetate was increased from 14 to 90 % with the increase of the amount of catalyst from 0.05 to 0.25 g per 2 mmol of alcohol, but further increasing did not improve the yield (Table 1, entries 1–6). The appropriate amount of catalyst in the reaction mixture was 0.25 g per 2 mmol of alcohol used, which resulted in the best yield (Table 1, entry 5). In order to choose the best medium, the reaction was also studied in some organic solvents such as acetonitrile, toluene, acetone and dichloromethane under refluxing conditions (Table 1, entries 7–10). As can be seen in Table 1, the best results in terms of reaction time and product yield have been achieved without the use of any solvent (18 min, 90 %). Therefore, we have continued the reactions under solvent-free conditions.

In an experiment, the pure (unsupported) LaFeO_3 nanoparticles were used as the catalyst for the acetylation

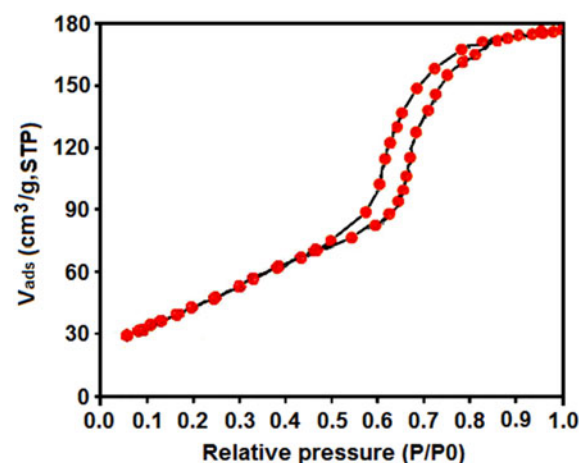


Fig. 4 Nitrogen adsorption–desorption isotherm curve for the $\text{LaFeO}_3/\text{SiO}_2$ nanocomposite prepared at $500\text{ }^\circ\text{C}$

Table 2 Results of acetylation of alcohols, phenols and amines with acetic anhydride over LaFeO₃/SiO₂ nanocomposite

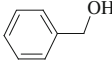
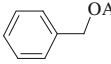
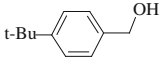
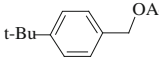
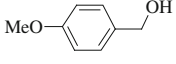
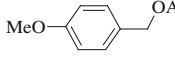
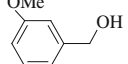
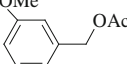
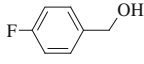
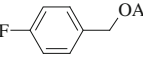
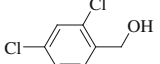
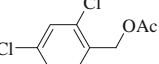
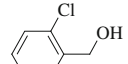
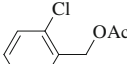
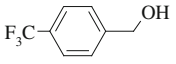
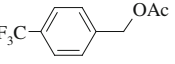
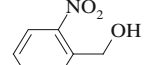
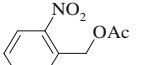
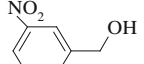
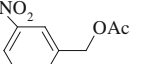
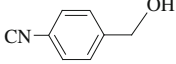
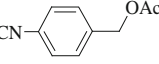
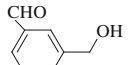
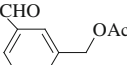
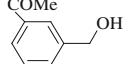
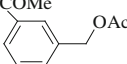
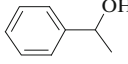
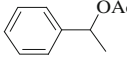
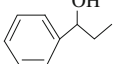
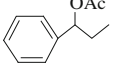
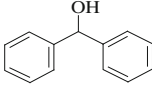
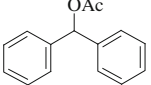
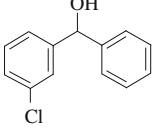
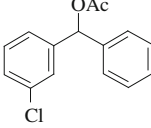
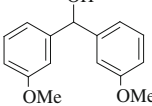
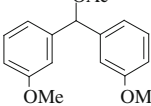
Entry	Substrate	Product ^b	Time (min)	Yield (%) ^c
1			18	90
2			12	92
3			10	91
4			12	88
5			18	86
6			18	90
7			19	88
8			22	86
9			20	85
10			20	86
11			22	85
12			20	85
13			20	87
14			16	92
15			16	90
16			12	92
17			15	90
18			14	92

Table 2 Results of acetylation of alcohols, phenols and amines with acetic anhydride over LaFeO₃/SiO₂ nanocomposite

Entry	Substrate	Product ^b	Time (min)	Yield (%) ^c
19			25	86
20			25	86
21			25	85
22			30	78
23			22	87
24 ^d			32	88
25			35	86
26			25	88
27			42	82
28			40	85
29			32	84
30			6	90
31			5	94
32			5	94
33			5	91
34			8	88
35			6	90
36			6	90

Reaction conditions: substrate (2 mmol), acetic anhydride (one equiv. per OH or NH₂ group), catalyst (0.25 g) under solvent-free conditions and at RT

^a All products were characterized on the basis of GC-MS, IR and ¹H-NMR spectral data

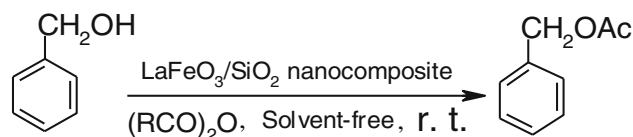
and comparison with those of authentic samples or reported data

^b Isolated yield on the basis of the weight of the pure product obtained

^c The reaction was carried out on a 20 mmol scale of benzyl alcohol

of benzyl alcohol under similar conditions. The result revealed that LaFeO₃ in the supported state is more active than the neat form (Table 1; entry 11). The amount of

LaFeO₃ (0.10 g) used in the reaction was approximately the same as the amount of the LaFeO₃ estimated to be present in 0.250 g of 40 % LaFeO₃/SiO₂ nanocomposite.

Table 3 Results of the protection of benzyl alcohol with various anhydrides over LaFeO₃/SiO₂ nanocomposite

Anhydride	Ac ₂ O	(EtCO) ₂ O	(iso-PrCO) ₂ O	(PhCO) ₂ O ^b
Time (min)	18	25	33	40
Yield (%) ^a	90	85	85	76

Reaction conditions: benzyl alcohol (2 mmol), anhydride (2 mmol), catalyst (0.25 g)

^a Isolated yield of the corresponding acylated product

^b 2 equiv of (PhCO)₂O was used

Benzyl acetate was the only product observed in both the cases. Using pure SiO₂ support as a catalyst, <5 % product was detected from GC analysis of the reaction mixture after 30 min (Table 1; entry 12), suggesting that the catalytic activity of the LaFeO₃/SiO₂ nanocomposite derives mainly from the LaFeO₃ nanoparticles. The essential role played by the nanocomposite catalyst is evident from the extremely low yield of benzyl acetate (<5 %) found in the absence of it (Table 1, entry 13).

The generality of this protocol is shown by utilizing various primary, secondary and tertiary alcohols, as well as an allylic alcohol and diols (Table 2). The results in Table 2 show that all substrates were selectively converted to the corresponding acetates in high yields without any evidence of the formation of side products. The acetylation of a wide range of ring-substituted primary benzyl alcohols having various electron-donating and electron-withdrawing groups was investigated with acetic anhydride over LaFeO₃/SiO₂ nanocomposite. These alcohols and also primary aliphatic alcohols were efficiently converted to their corresponding acetates with excellent yields, and the nature of the substituents had no significant effect on the reaction times and yields (Table 2, entries 1–13). In addition, various secondary alcohols were converted in high yields to their corresponding acetates (Table 2, entries 14–18). The α,β -unsaturated primary alcohol such as cinnamyl alcohol was selectively converted to the corresponding acetate, and the carbon–carbon double bond remained intact under the reaction conditions (Table 2, entry 19). In addition, non-benzylic primary alcohols were converted with high selectivity to their corresponding acetates with high efficiency under the same reaction conditions (Table 2, entries 20 and 21). A sterically hindered tertiary alcohol such as triphenylmethanol also can be acetylated with high yield, but it takes a longer reaction time (Table 2, entry 22). As shown by GC–MS analysis, there was no elimination product in the reaction mixture. The efficiency of the catalyst can be seen clearly in the acetylation of a di-hydroxy

compound under similar conditions (Table 2, entry 23). Among the various alcohols studied, secondary benzylic alcohols were found to be most reactive, giving the corresponding acetylated products within shorter reaction times. As we can see from Table 1, functional groups such as –OMe, –CHO, –COMe, –CN and –NO₂ remained unchanged under the reaction conditions. In addition, the conversion of benzyl alcohol into benzyl acetate on a 20-mmol scale proceeded just, as well as the 2-mmol reaction (32 min, 88 %) (Table 2, entry 24).

The acetylation of phenols was also investigated under the present experimental conditions. Phenol, substituted phenols with electron-donating and electron-withdrawing groups, α -naphthol and thiophenol were acetylated in high yields albeit within longer reaction times in comparison with alcohols (Table 2, entries 25–29). The excellent activity of the LaFeO₃/SiO₂ nanocomposite was demonstrated by the high yields obtained for *para*-nitrophenol with a strong electron-withdrawing group (Table 2, entry 27).

Under the optimized conditions, primary aromatic amines containing various electron-donating and -withdrawing groups were also treated with acetic anhydride. Excellent results were obtained in each case affording the corresponding acetylated derivatives in 88–94 % yields in 5–8 min at room temperature under solvent-free conditions (Table 2, entries 30–34). Selective acetylation of –NH₂ group in the presence of –OH group was observed at room temperature with one equivalent of acetic anhydride (Table 2, entries 35 and 36). Thus, acetylation of amino alcohols and amino phenols produced the corresponding acetamides as sole products; the hydroxyl moiety remained untouched. This might be due to more nucleophilicity of –NH₂ group than –OH group. The selective acetylation of a primary NH₂ over a primary OH by this process is of considerable synthetic importance and it is difficult to achieve with many other reagents.

The activity of LaFeO₃/SiO₂ nanocomposite as a general catalyst was tested via the protection of benzyl alcohol

Table 4 Recyclability of the catalyst

Cycle	0	1st	2nd	3rd	4th
Yield ^a (%)	90	90	88	85	80

Reaction conditions: benzyl alcohol (2 mmol), acetic anhydride (2 mmol), under solvent-free conditions at r.t.

^a Yields are for isolated pure product

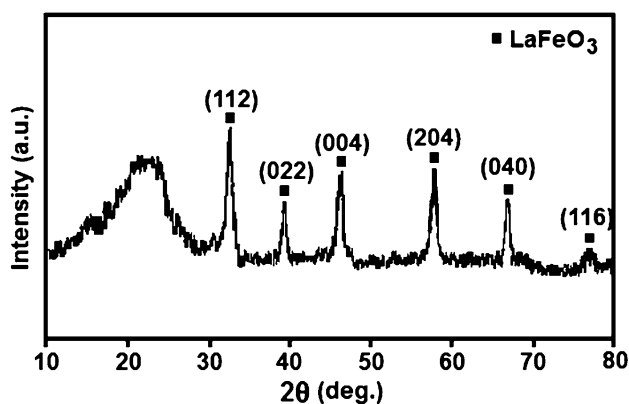


Fig. 5 XRD pattern of the recovered LaFeO₃ catalyst after the fourth run

with other anhydrides under same reaction conditions (Table 3). In comparison with acetic anhydride, the reactions with higher anhydrides took longer times at room temperature. However, the reactions were completed in 18–40 min under solvent-free conditions affording the corresponding acylated derivatives, providing excellent yields (76–90 %). It seemed that the rate of acylation was influenced by the steric and electronic factors of anhydrides and followed the order $\text{Ac}_2\text{O} > (\text{EtCO})_2\text{O} > ({}^i\text{PrCO})_2\text{O} > (\text{PhCO})_2\text{O}$. The longer times required for the reaction with $(\text{EtCO})_2\text{O}$ and $({}^i\text{PrCO})_2\text{O}$ were mainly due to the steric effect of the alkyl groups of these anhydrides. The longer reaction time and the requirement of two equivalents of $(\text{PhCO})_2\text{O}$ against one equivalent of Ac_2O were due to the combined effect of the steric and electronic factors of the phenyl group in $(\text{PhCO})_2\text{O}$. The phenyl group

makes the carbonyl group in $(\text{PhCO})_2\text{O}$ less electrophilic due to the resonance effect.

The recycling ability of the catalyst was tested in the acetylation of benzyl alcohol. After completion of the reaction, ethyl acetate was added and the mixture was filtered to separate the catalyst. The recycled catalyst was dried and used in further runs. No appreciable decrease in activity of the catalyst was observed even after fourth run (Table 4).

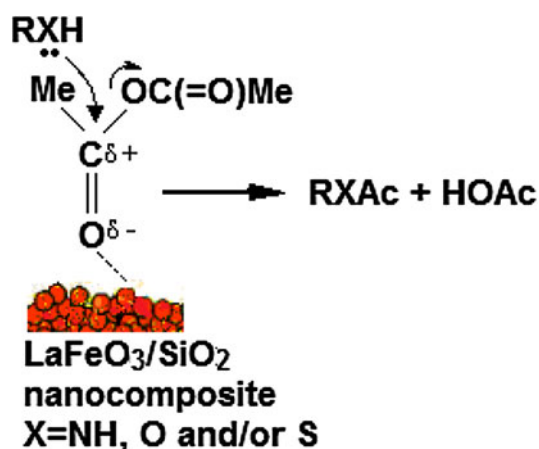
The nature of the recovered catalyst was also investigated by the XRD analyses. As shown in Fig. 5, the XRD pattern of the recovered catalyst did not show any significant change after fourth cycle compared to the fresh catalyst in Fig. 1, an indication that the structure of the LaFeO₃/SiO₂ nanocomposite was quite stable under the reaction conditions and was not affected by the reactants. In addition, the XRD pattern of the recovered catalyst revealed the absence of characteristic peaks of organic impurities.

To elucidate the advantages of the present method, we have compared the obtained results in the acetylation of benzyl alcohol with acetic anhydride over the LaFeO₃/SiO₂ nanocomposite with some reported heterogeneous catalysts in the literature (Table 5). It is clear that with respect to the reaction conditions, substrate:Ac₂O mole ratio, reaction time, and/or product yield, the present method is more suitable and/or superior. We can see that the reaction in the presence of most these catalysts required longer time for completion. Other advantages of the catalyst in this work in comparison with other previously reported catalysts are easy preparation, no moisture sensitivity, no explosive and expensive, and it has very low toxicity.

The mechanism for the acetylation of various substrates to their corresponding acetates using the LaFeO₃/SiO₂ nanocomposite has been proposed in Scheme 1 [27, 28]. As shown in the Scheme 1, at the initial stage, the carbonyl group of acetic anhydride is coordinated to the unsaturated La(III) and Fe(III) ions on the surface of the nanocomposite as Lewis acidic sites and then it was activated. The

Table 5 Comparison of the result obtained for the acetylation of benzyl alcohol in the present work with those obtained by some reported heterogeneous catalysts

Entry	Heterogeneous catalyst	Conditions	Alcohol:Ac ₂ O (mole ratio)	Catalyst (g)	Time (min)	Yield (%)	Ref.
1	Mont. KSF	Solvent-free, r.t.	1:2	0.1	60	90	[20]
2	SiO ₂ /H ₂ SO ₄	CH ₂ Cl ₂ , r.t.	1:2	0.2	240	90	[22]
3	FER zeolite	Solvent-free, 75 °C	1:1.5	0.15	120	91	[24]
4	Sulphated ZrO ₂	Solvent-free, r.t.	1:1	0.05	10	93	[28]
5	(NH ₄) _{2.5} H _{0.5} PW ₁₂ O ₄₀	Solvent-free, r.t.	1:1	0.5	60	92	[29]
6	Rice husk	Solvent-free, 80 °C	1:3	0.3	60	94	[37]
7	LaFeO ₃ /SiO ₂	Solvent-free, r.t.	1:1	0.25	18	90	This work



Scheme 1 The catalytic pathway for the acetylation reaction over the LaFeO₃/SiO₂ nanocomposite

activated carbonyl group reacts with substrate to give the corresponding acetate.

In a similar manner with other heterogeneous catalytic reactions, this reaction also takes place mainly on the surface of the catalyst, and surface atoms make a distinct contribution to its catalytic activity. In fact, the surface atoms behave as the Lewis acid centers where the chemical reaction could be catalytically activated. On the other hand, the number of surface atoms in the nanocomposite is a larger fraction of the total and provides more contact area for the reactants and the catalyst mainly due to its high surface-to-volume ratio and high surface area as compared with bulk particles. Therefore, the higher catalytic activity of LaFeO₃ in the nanocomposite than the pure LaFeO₃ can be attributed to the better coordination of the carbonyl group to the LaFeO₃/SiO₂ nanocomposite due to more surface Lewis acidic sites, participating at the reaction.

Conclusions

In conclusion, in this paper LaFeO₃/SiO₂ nanocomposite prepared by the sol-gel method was successfully applied as a novel, efficient and recyclable heterogeneous catalyst for the acetylation of alcohols, phenols and amines with acetic anhydride under solvent-free conditions. Among the various substrates, acetylation of amines was preceded rapidly, therefore selective acetylation of -NH₂ group in the presence of -OH group was observed. The LaFeO₃/SiO₂ nanocomposite was easily prepared and reusable without the loss of activity. XRD data showed that the structure of the catalyst did not change after the reaction. We described the acetylation of alcohols, phenols and amines with acetic anhydride over the LaFeO₃/SiO₂ nanocomposite catalyst in this paper for the first time.

Acknowledgments The authors gratefully acknowledge the Lorestan University Research Council and Iran Nanotechnology Initiative Council (INIC) for their financial support.

References

- J.R. Hanson, *Protecting Groups in Organic Synthesis*, 1st edn. (Blackwell Science Inc., Malden, MA, 1999)
- T.W. Greene, P.G.M. Wuts, *Protective Groups in Organic Synthesis*, 3rd edn. (Wiley, New York, 1999)
- A. Orita, C. Tanahashi, A. Kakuda, J. Otera, *Angew. Chem., Int. Ed.* **39**, 2877–2879 (2000)
- Y. Nakae, I. Kusaki, T. Sato, *Synlett* **10**, 1584–1586 (2001)
- K.L. Chandra, P. Saravanan, R.K. Singh, V.K. Singh, *Tetrahedron* **58**, 1369–1374 (2002)
- R. Dalpozzo, A.D. Nino, L. Maiuolo, A. Procopio, M. Nardi, G. Bartoli, R. Romeo, *Tetrahedron Lett.* **44**, 5621–5624 (2003)
- A.K. Chakraborti, R. Gulhane, *Tetrahedron Lett.* **44**, 6749–6753 (2003)
- [8] G. Bartoli, M. Bosco, R. Dalpozzo, E. Marcantoni, M. Massaccesi, S. Rinaldi, L. Sambri, *Synlett* (2003) 39–42
- [9] G. Bartoli, M. Bosco, R. Dalpozzo, E. Marcantoni, M. Massaccesi, L. Sambri, *Eur. J. Org. Chem.* (2003) 4611–4617
- S.K. De, *Tetrahedron Lett.* **45**, 2919–2922 (2004)
- P. Phukan, *Tetrahedron Lett.* **45**, 4785–4787 (2004)
- M.H. Heravi, F.K. Behbahani, F.F. Bamoharram, *J. Mol. Catal. A: Chem.* **253**, 16–19 (2006)
- M. Moghadam, S. Tangestaninejad, V. Mirkhani, I. Mohamadpoor-Baltork, S.A. Taghavi, *J. Mol. Catal. A: Chem.* **274**, 217–223 (2007)
- G. Sartori, R. Ballini, F. Bigi, G. Bosica, R. Maggi, P. Righi, *Chem. Rev.* **104**, 199–250 (2004)
- A. Sakakura, K. Kawajiri, T. Ohkubo, Y. Kosugi, K. Ishihara, *J. Am. Chem. Soc.* **129**, 14775–14779 (2007)
- A.K. Chakraborti, R. Gulhane, *Chem. Commun.* **22**, 1896–1897 (2003)
- T.-S. Li, A.-X. Li, *J. Chem. Soc., Perkin Trans.* **1**, 1913–1917 (1998)
- [18] A.-X. Li, T.-S. Li, T.-H. Ding, *Chem. Commun.* (1997) 1389–1390
- M.L. Kantam, K.V.S. Ranganath, M. Sateesh, B. Sreedhar, B.M. Choudary, *J. Mol. Catal. A: Chem.* **244**, 213–216 (2006)
- M.H. Sarvari, H. Sharghi, *Tetrahedron* **61**, 10903–10907 (2005)
- H.T. Thakuria, B.M. Borah, G. Das, *J. Mol. Catal. A: Chem.* **274**, 1–10 (2007)
- F.M. Moghaddam, H. Saeidian, *Mater. Sci. Eng. B* **139**, 265–269 (2007)
- F. Shirini, M.A. Zolfigol, K. Mohammadi, *Bull. Korean Chem. Soc.* **25**, 325–327 (2004)
- R. Ballini, G. Bosica, S. Carloni, L. Ciaralli, R. Maggi, G. Sartori, *Tetrahedron Lett.* **39**, 6049–6052 (1998)
- S.P. Chavan, R. Anand, K. Pasupathy, B.S. Rao, *Green Chem.* **3**, 320–322 (2001)
- A.K. Chakraborti, R. Gulhane, *Tetrahedron Lett.* **44**, 3521–3525 (2003)
- J.K. Joseph, S.L. Jain, B. Sain, *J. Mol. Catal. A: Chem.* **267**, 108–111 (2007)
- B. Das, P. Thirupathi, *J. Mol. Catal. A Chem.* **269**, 12–16 (2007)
- K.J. Ratnam, R.S. Reddy, N.S. Sekhar, M.L. Kantam, F. Figueras, *J. Mol. Catal. A: Chem.* **276**, 230–234 (2007)
- J.R. Satam, R.V. Jayaram, *Catal. Commun.* **9**, 2365–2370 (2008)
- F. Rajabi, *Tetrahedron Lett.* **50**, 395–397 (2009)
- K. Niknam, D. Saberi, *Tetrahedron Lett.* **50**, 5210–5214 (2009)
- K. Niknam, D. Saberi, *Appl. Catal. A: Gen.* **366**, 220–225 (2009)

34. N. Ghaffari-Khaligh, *J. Mol. Catal. A: Chem.* **363–364**, 90–100 (2012)
35. A. Rahmatpour, *Comptes Rendus Chimie* **15**, 1048–1054 (2012)
36. L. Osiglio, Á.G. Sathicq, G.P. Romanelli, M.N. Blanco, *J. Mol. Catal. A: Chem.* **299**, 97–103 (2012)
37. F. Shirini, S. Akbari-Dadamahaleh, A. Mohammad-Khah, A.R. Aliakbar, *Comptes rendus chimie* in press, Corrected Proof. Accessed 23 May 2013
38. R. Spinicci, M. Faticanti, P. Marini, S. Derossi, P. Porta, *J. Mol. Catal. A: Chem.* **197**, 147–155 (2003)
39. B.P. Barbero, J.A. Gamboa, L.E. Cadus, *Appl. Catal. A: Environ.* **65**, 21–30 (2006)
40. N.A. Merino, B.P. Barbero, P. Ruiz, L.E. Cadus, *J. Catal.* **240**, 245–257 (2006)
41. H. Grabowska, W. Mista, M. Zawadzki, J. Wrzyszczyk, *Polish J. Chem. Technol.* **5**, 32–34 (2003)
42. S. Farhadi, S. Panahandehjoo, *Appl. Catal. A: Gen.* **382**, 293–302 (2010)
43. S. Farhadi, M. Zaidi, *J. Mol. Catal. A: Chem.* **299**, 18–25 (2009)
44. J.D. Wright, N.A.J.M. Sommerdijk, *Sol–Gel Materials: Chemistry and Applications* (Taylor & Francis, UK, 2001)
45. C. Cannas, A. Musinu, D. Peddis, G. Piccaluga, *Chem. Mater.* **18**, 3835–3842 (2006)
46. C. Cannas, A. Ardu, D. Niznansky, D. Peddis, G. Piccaluga, A. Musinu, *J. Sol–Gel Sci. Technol.* **60**, 266–274 (2011)
47. M. Barbu, M. Stefanescu, M. Stoia, G. Vlase, P. Barvinschi, *J. Therm. Anal. Calorim.* **108**, 1059–1066 (2012)
48. X. Wang, M.V. Landau, H. Rotter, L. Vradman, A. Wolfson, A. Erenberg, *J. Catal.* **222**, 565–571 (2004)
49. S. Farhadi, F. Siadatnasab, *J. Mol. Catal. A: Chem.* **339**, 108–116 (2011)
50. B.D. Cullity, S.R. Stock, *Elements of X-ray Diffraction*, 3rd edn. (Prentice-Hall, Englewood Cliffs, New Jersey, 2001)
51. X.L. Duan, D.R. Yuan, D. Xu, M.K. Lu, X.Q. Wang, Z.H. Sun, Z.M. Wang, H.Q. Sun, Y.Q. Lu, *Materials Research Bulletin* **38**, 705–711 (2003)
52. S.M. Khetrea, A.U. Chopadea, C.J. Khilarea, S.R. Bamane, *Int. J. Porous Mater.* **1**, 1–5 (2011)